Journal of Energy

VOLUME 61 Number 1–4 | 2012 Special Issue

journal homepage: http://journalofenergy.com/

Franjo Kelemen
Končar Power Transformers Ltd.
franjo.kelemen@siemens.com

Kosjenka Capuder
Končar Power Transformers Ltd.
kosjenka.capuder@siemens.com

Leonardo Štrac
Končar Power Transformers Ltd.
leonardo.strac@siemens.com

# SKIN – EFFECT LOSSES IN DIFFERENT LOADING CONDITIONS OF A POWER TRANSFORMER

## SUMMARY

The subject of the analysis is a 300 MVA auto-connected power transformer in different loading conditions with regard to the load losses. During the electrical design time, some operating points of the transformer were analyzed in more detail using 2D electromagnetic field finite element method (FEM) software. The models included 2D magnetic stray field calculation and covered a range of transformer loading cases that covered some that are more difficult to solve with traditional analytic methods based on the static magnetic field calculations. This is due to the presence of a phase shift between the currents through the windings. The results of the static magnetic Rabins' method field calculation and the FEM method are compared and the best practice method is defined and determined accordingly.

**Key words:** Finite element method, load losses, phase shift, power transformer, skin – effect.

## 1. INTRODUCTION

Load losses in a power transformer consist of different loss components. In general, these are the ohmic losses due to the winding and lead resistance, the skin-effect and proximity effect losses [1] in windings due to the stray field and additional losses outside of windings in the metal parts of transformer. As all these components add-up together in each case of the transformer load, the calculation of the stray flux density field distribution and, consequently, the losses is the first step to be taken. The usual approach in losses calculation is to use the 2D cylindrical coordinate system and Rabins' method [1] to model the stray field distribution. However, this method relies on static magnetic field distribution and needs to have a balance of ampere-turns on the transformer-leg to be applied correctly within the scope of the method. When there is a phase shift present in the winding currents, although the net sum of ampere turns in each time instance is still zero, the magnitudes of currents can not be directly fed to the mathematical model and used without some modifications. This is why the 2D FEM solver is applied to test the range or feasibility of application of Rabins' method in power transformer design. The inherent drawback of the quasistatic calculation of the losses in conductor strands is in its need of high number of elements to represent the geometry in a correct manner. The number of elements is in direct correlation with execution time of the calculation process and makes the usage of FEM less feasible in comparison with analytic methods.



F. Kelemen, K. Capuder, L. Štrac, Skin – effect losses in different loading conditions of a power transformer, Journal of Energy, vol. 61 Number 1–4 (2012) Special Issue, p. 107-112

https://doi.org/10.37798/2012611-4242

## 2. MAGNETIC STRAY FIELD DISTRIBUTION IN A POWER TRANSFORMER DURING DIFFERENT LOADING CONDITIONS

The power transformer must be capable of continuous service in all normal operational points. However, different loading conditions change the distribution of the ampere turns in the transformer winding geometry. Hence, the additional losses along with skin-effect and proximity effect losses that are primarily influenced by the distribution of the stray field will also vary. The cooling system must be capable of exchanging the heat between the transformer and the environment, keeping the temperatures of the transformer copper and iron in the acceptable range. Therefore, the relevant loading case has to be found with respect to the load loss and additional losses. The stray field of a transformer, or the magnetic induction distribution in the transformer, is a function of the current excitation through the windings. Traditional methods only use analytic static magnetic field solution [1], [2] inside the core window based on the Rabins' method. The choice of operating points is made with maximum load losses in mind (see Table I). The graphical representation of the spatial 2D distribution of the magnitude of the magnetic induction vector field in cylindrical coordinate system is shown in the Fig. 1 for three normal (operating points without the phase shift between the currents) and one with the phase shift (cases correspond to ones given respectively in Table I).

Table I Load cases considered.

| Loading condition | $I_{TV}$ in A | $I_{FR1}$ in A | $I_{FR2}$ in A | $I_P$ in A | $I_S$ in A |
|---|---|---|---|---|---|
| HV/LV(+) | 0 | $1120\angle 0°$ | $1120\angle 0°$ | $687\angle 0°$ | $433\angle 0°$ |
| HV/LV (0) | 0 | $1312\angle 0°$ | $1312\angle 0°$ | $879\angle 0°$ | $433\angle 0°$ |
| HV/LV (-) | 0 | $1584\angle 0°$ | $1584\angle 0°$ | $1151\angle 0°$ | $433\angle 0°$ |
| HV/LV/TV | $2436\angle 90°$ | $1121\angle -3.31°$ | $1121\angle -3.31°$ | $763\angle -14.38°$ | $400\angle 18.18°$ |

The final load case from the table I is illustrated in Fig. 1 d) and is represented graphically with complex magnitude of the vector of magnetic induction, or

$$\max_{t,\varphi}(B(r,\theta,z,\omega t-\varphi)) \text{ for each } \forall r,\theta,z \tag{1}$$

Calculated ohmic losses are given in the table II. The ohmic losses are only one part of the total losses and calculated directly, while the additional losses are estimated through the stray flux in a certain tap position of the power transformer. Due to the fact that stray flux entering the conductive parts of a transformer is directly connected to the stray losses, different estimation formulae are constructed to emulate the behavior of the stray losses with respect to the stray flux level. Usually, the losses are modeled through the portion of the flux entering the conductive materials. While the currents are of the same phase angle, the distribution of the stray field in connection with the additional losses estimation can be done through the results at a single time instant. However, when the phase shift between the load currents is present, the stray flux distribution changes in time (the character of the distribution changes). Consequently, the overall local maxima in stray flux distribution have to be found, the reduced stray flux curves need to be calculated and only then is the estimation of the stray losses possible using the same principles as in the other cases of operation. The illustration of the basic idea of additional (stray) losses estimation is presented in figure 2. The (axial component of) magnetic flux density distribution through the middle of the windings, the stray flux and reduced stray flux integral curves are given as a visual representation of the stray losses in different tap positions and operating points.

Table II Ohmic loss in different loading conditions.

| Configuration | T ohmic loss in kW/phase | FR ohmic loss in kW/phase | LV ohmic loss in kW/phase | HV ohmic loss in kW/phase | Total ohmic loss in kW |
|---|---|---|---|---|---|
| HV-LV(+) | 1.7 | 13.5 | 49.8 | 126.7 | 575.0 |
| HV-LV(0) | 0.3 | 0.1 | 70.8 | 126.7 | 593.7 |
| HV-LV(-) | 0.4 | 25.9 | 115.1 | 126.8 | 804.8 |
| HV-LV(1)-T | 36.6 | 4.5 | 56.1 | 105.0 | 606.6 |

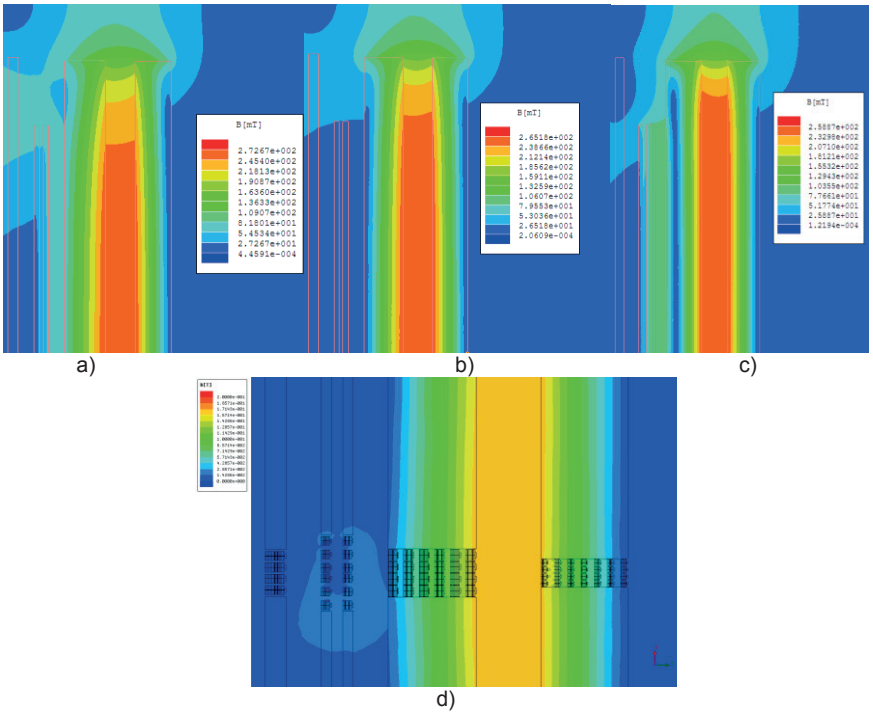


Fig. 1 Distribution of the magnitude of the magnetic induction vector (complex magnitude) on the 2D axisymmetric geometry of a power transformer; a) HV/LV(+); b) HV/LV (0); c) HV/LV (-); d) HV/LV/TV loading condition.

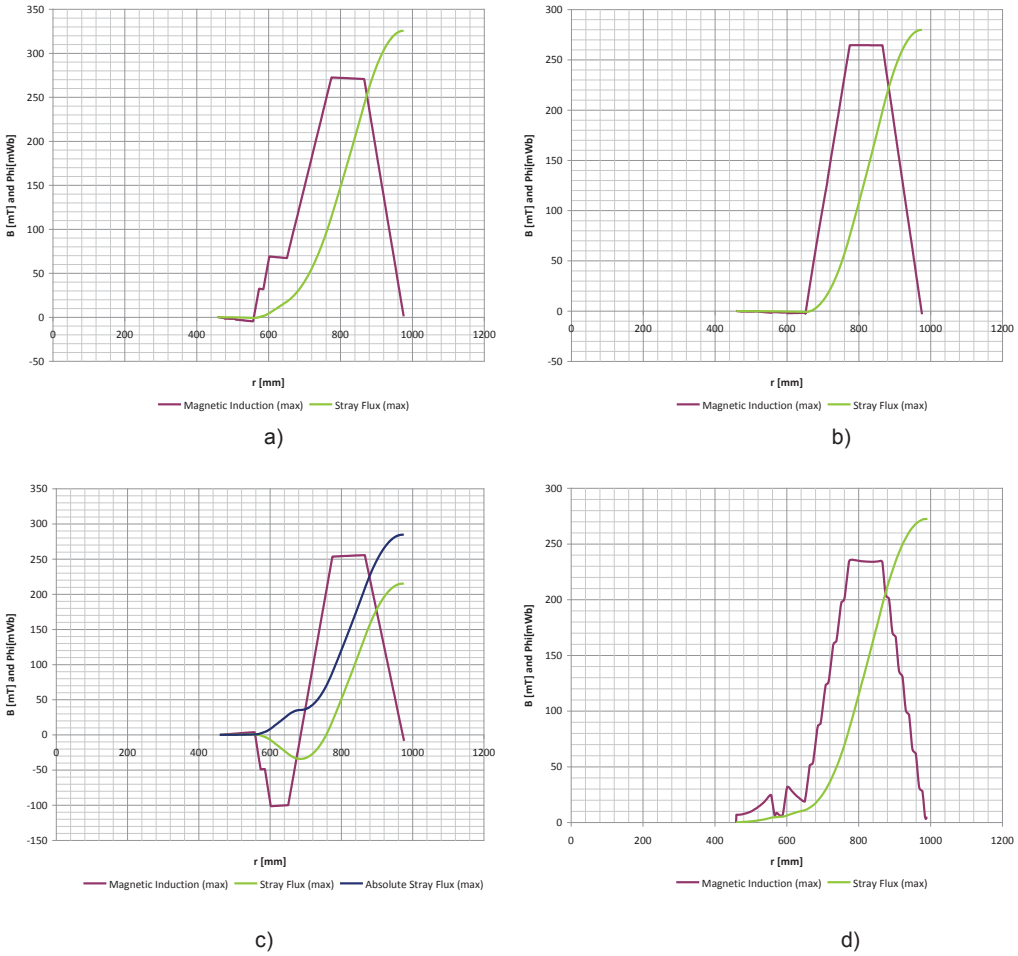


Fig. 2 Axial magnetic induction distribution (complex magnitude) in the radial direction in the plane of the symmetry of the winding heights during different loading conditions; a) HV/LV(+); b) HV/LV (0); c) HV/LV (-); d) HV/LV/TV.

The stray flux lines of the transformer stray field have predominantly axial component (see Fig. 1) in the middle of the winding and for the most of the winding height. At the top and bottom of the winding, the stray flux lines gain the radial component. Therefore, the winding can be effectively subdivided in two regions, one with predominant radial skin-effect and one with the axial skin-effect. The skin-effect calculation requires that each strand of the continuously transposed conductor (CTC) is modeled. As the radial flux density field is strongest at the winding ends, it is enough to model 5-10% of the winding height in more detail. The other part of the winding that needs to be represented in more detail is the middle of the winding, where the axial skin-effect is the strongest. Subdivisions that allow the simplification of geometry are presented in Fig. 3.

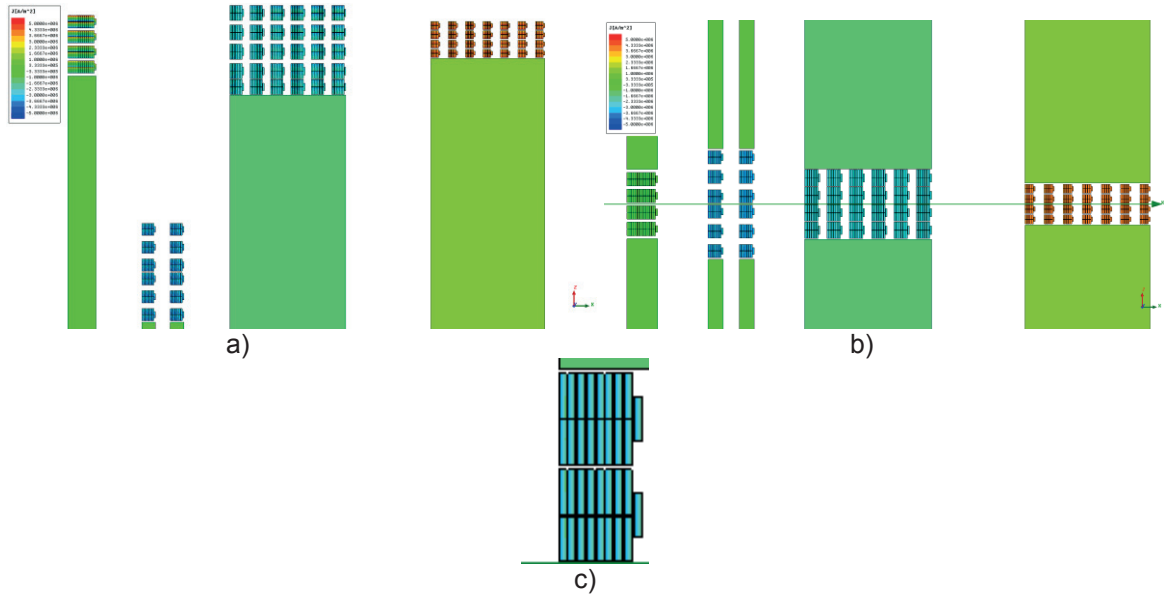


Fig. 3 FEM model of the winding end a), winding middle b) and a detail of CTC conductor array modeled c).

It is fairly easy to recognize that the calculation process with high detailed windings using FEM takes significantly higher amount of time to be completed than using analytic method. Therefore, the previous knowledge of the stray flux behavior is used to simplify the calculations and model only the regions that are notably different with respect to losses calculation. The overall losses are then calculated using the results obtained through the regions.

## 3. ANALYTICAL APPROACH

With some modifications, analytical method can still be applied in the cases of phase shift between the winding load currents. The key is to model two different time instants that differ by 90° degrees electrical. To test the applicability of the approach, elaborate models based on 2D magnetic FEM quasistatic field solution are used first to confirm the overall quality of the skin-effect calculation by traditional methods and then to scrutinize the "new" approach that broadens the spectrum of application of the analytical software currently in use. Based on the magnetic field density vector fields obtained in the calculation, additional losses are estimated and skin-effect losses are calculated.

Total power in the windings is calculated using:

$$p_{tot}(t) = p_1(t) + p_2(t) + \ldots + p_n(t) \tag{2}$$

In (2), $p_{tot}(t)$ is a time function of power, where $p_1(t),\ldots, p_n(t)$ are components of power in respective windings. These components of power are obtained through the set of equations:

$$\begin{aligned} p_1(t) &= u_1(t)\cdot i_1(t) \\ &\vdots \\ p_n(t) &= u_n(t)\cdot i_n(t) \end{aligned} \tag{3}$$

where: $u_1(t)$, …, $u_n(t)$ denote the voltages and
$i_1(t)$, …, $i_n(t)$ are currents at a time instant $t$.
Specifically, in the case of simple harmonic functions of voltage and current the following holds:

$$p_1(t) = U_1 \sin \omega t \cdot I_1 \sin(\omega t - \phi_1) = U_1 I_1 \frac{\cos\phi_1 - \cos(2\omega t - \phi_1)}{2}, \quad (4)$$

Where: $U_1$ and $I_1$ are peak values of voltage and current,
ω is the angular frequency (ω=2π$f$),
$\varphi_1$ is the phase shift between voltage and current waveforms,
$f$ is the line frequency.
The mean value of $p_1$ represents ohmic losses, $P_{mean1}$, which can be expressed using relation (5).

$$P_{mean1} = \overline{p_1(t)} = \frac{U_1 I_1 \cos\phi_1}{2} \quad (5)$$

In general, for each argument α, $p_1(\alpha)$ can be expressed as in (6).

$$p_1(\alpha) = U_1 \sin \omega\alpha \cdot I_1 \sin(\omega\alpha - \phi_1) = U_1 I_1 \frac{\cos\phi_1 - \cos(2\omega\alpha - \phi_1)}{2} \quad (6)$$

It is convenient to proceed with calculation for the time instant that differs by 90° degrees electrical, i.e. time instants $p_1(\alpha)$ and $p_2(\alpha+\pi/2)$:

$$\begin{aligned} p_2\left(\alpha + \frac{\pi}{2}\right) &= U_1 \sin\left(\omega\alpha + \frac{\pi}{2}\right) \cdot I_1 \sin\left(\omega\alpha + \frac{\pi}{2} - \phi_1\right) \\ &= U_1 I_1 \frac{\cos\phi_1 - \cos(2\omega\alpha + \pi - \phi_1)}{2} = U_1 I_1 \frac{\cos\phi_1 + \cos(2\omega\alpha - \phi_1)}{2} \end{aligned} \quad (7)$$

Careful inspection of relations (6) and (7) reveals that the arithmetic average of these two respective functions equals to (5). Therefore, their mean value $P_{mean}$ can be modeled using the respective powers calculated in two different time instances that are 90 electrical degrees apart, regardless of the initial parameter α. So, without losing the generality, the parameter α can be chosen arbitrarily and is usually set to zero.

$$P_1(\alpha) + P_2\left(\alpha + \frac{\pi}{2}\right) = U_1 I_1 \cos\phi_1 \quad (8)$$

$$P_{mean1} = \frac{P_1(\alpha) + P_2\left(\alpha + \frac{\pi}{2}\right)}{2} = U_1 I_1 \frac{\cos\phi_1}{2} \quad (9)$$

The important result written in the formula (9) that gives the total mean power (or losses), that is in fact independent of parameter α, allows the calculation of the losses in all possible cases of current distributions and phase shifts in the windings because the same holds true for $P_{mean2}$, $P_{mean3}$,...,$P_{meann}$. Using the developed approach, the losses in windings for the loading conditions with the phase shift between the currents are calculated. The results are given in the table III for each of the main windings and overall for one phase of a transformer.

Table III Ohmic losses in main windings and overall per phase losses calculated using FEM and Rabins' method for the case 4 in Table I.

| | LV ohmic loss in W/phase | HV ohmic loss in W/phase | Total ohmic loss in W/phase |
|---|---|---|---|
| Analytic method | 55251 | 105670 | 202569 |
| FEM | 56067 | 105013 | 202185 |
| Difference | -1.48% | 0.62% | 0.19% |

In table IV all the results of the calculated losses are compared using relative and absolute differences with respect to FEM calculation.

Table IV Ohmic loss in different loading conditions calculated using FEM and Rabins' method.

| Configuration | Total ohmic loss FEM in kW | Total ohmic loss - analytic in kW | Absolute differences in kW | Relative differences in % |
|---|---|---|---|---|
| HV-LV(+) | 575.0 | 575.5 | 0.50 | 0.09 |
| HV-LV(0) | 593.7 | 594.1 | 0.40 | 0.07 |
| HV-LV(-) | 804.8 | 805.8 | 1.00 | 0.12 |
| HV-LV(1)-T | 606.6 | 607.7 | 1.10 | 0.18 |

## 4. CONCLUSION

The comparison of results presented in previous chapter confirms that the simple Rabins' method used in calculation of the stray field and skin-effect losses in the windings can be used in more general scenarios with currents with shifted phase angles. The differences between the FEM method and analytic method in the results in such cases are below 0.2% and can be neglected. The major part of these differences is a byproduct of the numerical inaccuracy of the methods used in respective approaches. The analytic method of calculation is more practical with respect to the execution time of the process and therefore more suitable for usage in different optimization schemes.

## BIBLIOGRAPHY

[1] R. M. Del Vecchio, B. Poulin, P.T. Feghali, D. M. Shah, R. Ahuja, "Transformer Design Principles", Gordon and Breach Science Publishers, p. 149-184.

[2] Z. Haznadar, Ž. Štih, "Electromagnetic Fields, Waves and Numerical Methods", IOS Press, Amsterdam, Berlin, Oxford, Tokyo, Washington, 2000.